Continuous ambulatory hand force monitoring during manual materials handling using instrumented force shoes and an inertial motion capture suit

Faber GS[1,2,3*], Koopman AS[1], Kingma I[1], Chang CC[3,4], Dennerlein JT[2,5], van Dieën JH[1].

[1] Department of Human Movement Sciences, Faculty of Behavioural and Movement Sciences, Vrije Universiteit Amsterdam, Amsterdam Movement Sciences, Amsterdam, The Netherlands
[2]Department of Environmental Health, Harvard T.H. Chan School of Public Health, Boston, MA, USA
[3]Liberty Mutual Research Institute for Safety, Hopkinton, MA, USA
[4]Department of Industrial Engineering & Engineering Management, National Tsing Hua University, Taiwan, ROC
[5]Department of Physical Therapy, Movement, and Rehabilitation Sciences, Northeastern University, Boston, MA, USA

Word count: 3184

Keywords

- Wearable sensors;
- Occupational biomechanics;
- Ergonomics;
- Inertial measurement unit (IMU);
- Spine

*Corresponding Author:
Tel. : +31 20 59 88566
E-mail : gertfaber.sci@gmail.com
Fax : +31 20 59 88529

Abstract

Hand forces (HFs) are commonly measured during biomechanical assessment of manual materials handling; however, it is often a challenge to directly measure HFs in field studies. Therefore, in a previous study we proposed a HF estimation method based on ground reaction forces (GRFs) and body segment accelerations and tested it with laboratory equipment: GFRs were measured with force plates (FPs) and segment accelerations were measured using optical motion capture (OMC). In the current study, we evaluated the HF estimation method based on an ambulatory measurement system, consisting of inertial motion capture (IMC) and instrumented force shoes (FSs).

Sixteen participants lifted and carried a 10-kg crate from ground level while 3D full-body kinematics were measured using OMC and IMC, and 3D GRFs were measured using a FPs and FSs. We estimated 3D hand force vectors based: 1) FP+OMC, 2) FP+IMC and 3) FS+IMC. We calculated the root-mean-square differences (RMSDs) between the estimated HFs to reference HFs calculated based on crate kinematics and the GRFs of a FP that the crate was lifted from.

Averaged over subjects and across 3D force directions, the HF RMSD ranged between 10-15N when using the laboratory equipment (FP+OMC), 11-18N when using the IMC instead of OMC data (FP+IMC), and 17-21N when using the FSs in combination with IMC (FS+IMC). This error is regarded acceptable for the assessment of spinal loading during manual lifting, as it would results in less than 5% error in peak moment estimates.

1. Introduction

Manual materials handling studies often measure hand forces to assess load magnitudes and/or to calculate the related joint loads. In the laboratory, hand forces can be directly measured by instrumenting objects to be lifted (Dennis and Barrett, 2002; Plamondon et al., 1996). However, it is not feasible to instrument every object to be lifted in the actual workplace. One alternative is to use load sensing handles that workers use to lift boxes (Marras et al., 2010), but this may influence the natural movement pattern and still has limited applicability. Another option is to estimate hand forces from object mass and hand motion, but this requires monitoring of when and what subjects are lifting through laborious video observation methods (Coenen et al., 2011; Coenen et al., 2013).

Because of the above limitations, we have previously proposed a method to estimate 3D dynamic hand forces by calculating the difference between the ground reaction force (GRF) and the forces resulting from the mass and acceleration of all body segments (Faber et al., 2013a). As a proof of principle, the performance of this method was tested using laboratory equipment: GRFs were measured using a force plate (FP) and segment kinematics (accelerations) were measured using and optical motion capture (OMC) system. Errors in the estimated hand forces were around 20N which was regarded acceptable for assessment of spinal loading.

For application of this method in the actual workplace, GRFs and segment accelerations should be measured using ambulatory measurement tools. In previous studies, we have examined the applicability of measuring GRF using instrumented force shoes (FS) (Faber et al., 2009b) and segment accelerations using a full-body inertial motion capture (IMC) system consisting of inertial measurement units (IMUs) (Faber et al., 2015). In the present study, we evaluated the performance of these ambulatory measurement tools for the estimation of 3D hand forces. Because gender differences in anthropometry (de Leva, 1996) and lifting strategy (Plamondon et al., 2017) might affect system performance, both men and women were tested.

2. Methods

Eight male (age: 31±7years, mass: 77±13kg, height: 176±10cm) and eight female (age: 33±13years, mass: 61±3kg, height: 166±5cm) subjects participated in the experiment that was approved by institutional review boards of the Harvard T.H. Chan School of Public Health and the Liberty Mutual Research Institute for Safety. After providing written consent, subjects were equipped with all the measurement instrumentation and calibration measurements were done (see following sections). Subsequently subjects started the experimental trials in which they lifted/carried a 10kg crate (WxDxH: 33x33x28cm, of which the handles were positioned at 45 cm horizontal distance (handle height 25cm) from the FPs that the subjects were standing on during the lifts (the black plates in figure 1).

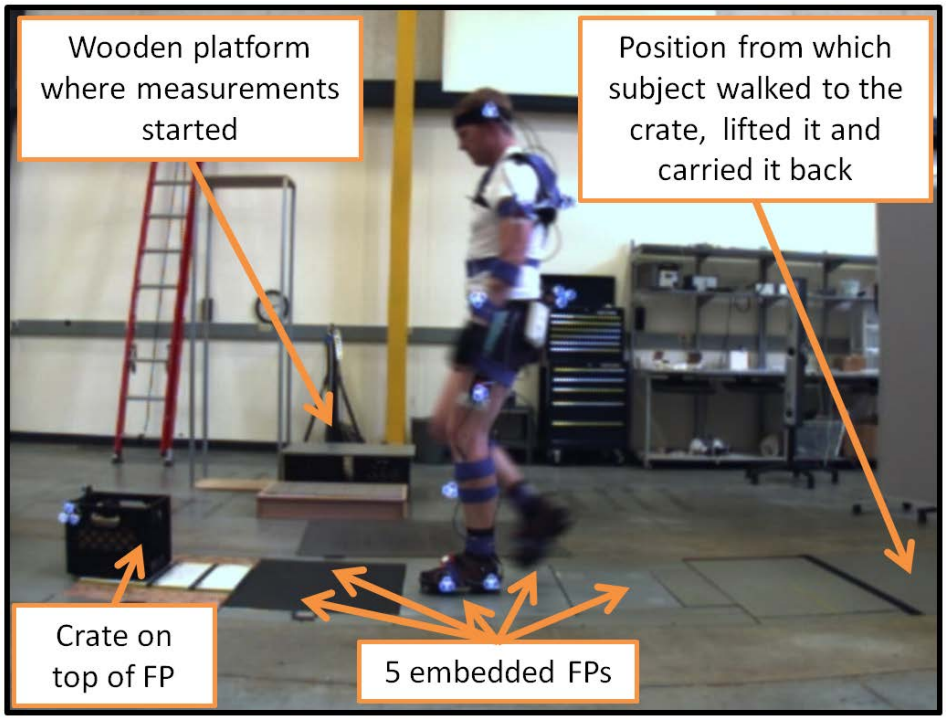

Fig. 1. *Photo of a subject walking toward the box during an experimental trial. To minimize effects of magnetic distortion at the beginning of the trial, measurements started while the subjects stood on a wooden platform to the side of the measurement volume. Subsequently, subjects walked to a position behind the force plates (FPs) from where they performed the crate lifting/carrying tasks. In each task, subjects performed the following subtasks: 1) walking over five floor-embedded FPs, 2) lifting the crate, and 3) turning and carrying the crate back to the initial position behind the FPs.Subjects and experimental procedures*

To minimize effects of magnetic distortion on the IMC recordings at the beginning of the trial, measurements started while the subjects stood on a wooden platform to the side of the measurement volume. Subsequently, subjects walked to a position behind the FPs from where they performed the crate lifting/carrying tasks. In each task, subjects performed the following subtasks:

1. walking over five floor-imbedded FPs,
2. lifting the crate,
3. turning and carrying the crate back to the initial position next to the FPs.

2.1. Instrumentation and data pre-processing

2.1.1. Full body kinematics

Full-body kinematics were measured with a Certus Optotrak OMC system at 50 samples/s (Northern Digital, Waterloo ON, Canada) and with an Xsens IMC system at 120 samples/s (MVN, Xsens technologies B.V., Enschede, the Netherlands).

For the IMC system, the standard full-body MVN setup was used (Kim and Nussbaum, 2013; Roetenberg et al., 2013) consisting of 17 IMUs. Data were recorded using Xsens software (MVN Studio 3.0, Xsens technologies B.V., Enschede), providing a built-in anatomical human body model. For the OMC system, marker clusters were used to capture segment motion.

Motion sensors (IMUs and marker clusters) were attached to the pelvis, head, the upper arms, forearms, thighs, shanks, and feet. In addition, marker clusters were placed on the posterior side of the thorax and the crate; and in accordance with the requirements of the built-in anatomical model, IMUs were placed on both scapulae, the sternum and hands. Because most marker clusters were attached to the inertial sensors, only non-magnetic material was used in the cluster structures.

2.1.2. Ground reaction Forces (GRFs)

GRF were measured with 6 Kistler FPs at 200 samples/s (Kistler Instrumente AG, Winterthur, Switzerland) and instrumented “ForceShoes” at 100 samples/s (FS, Xsens Technologies, Netherlands)

(Faber et al., 2009b; Liedtke et al., 2007; Schepers et al., 2007; Veltink et al., 2005). Each FS contained two force/torque sensors (FTsensor), one underneath the heel and one underneath the forefoot. Each FTsensor had an IMU attached to it, to measure its orientation, such that the locally measured forces could be rotated to the global coordinate system (Figure 2). Before the measurement each FTsensor was calibrated using a FP (Faber et al., 2012).

Fig. 2. *Overview of the ambulatory measurement system used in the present study (Xsens technologies B.V., Enschede). (A) Picture of one of the instrumented force shoes (FSs). (B) 3D representation of the force/torque and IMU sensors, and mounting plates underneath each FS. (C) Full-body inertial motion capture (IMC) system.*

2.1.3. Data pre-processing & synchronization

First, all force (FP & FS) and kinematic (OMC & IMC) data were resampled to 120 samples/s using linear interpolation. Subsequently, forces and kinematics were bi-directionally low-pass filtered with a second-order Butterworth filter at 10Hz and 5Hz, respectively. With respect to data synchronization, FP and OMC data were synchronously measured on one computer, IMC data were synchronized off-line

by using a cross-correlation procedure based on the resultant angular velocity of the head segment measured with the OMC and IMC, and for FS data synchronization, the same was done but then based on the angular velocity of the left heel.

2.2. Reference hand forces

As a reference, we calculated the 3D reference hand forces ($\mathbf{F_{HANDreference}}$) for each sample, based on the crate mass (m_{crate}) and CoM acceleration ($\mathbf{a}_{\boldsymbol{crate}}$), and the GRF measured by the FP that the crate was lifted from ($\mathbf{F_{GRFcrate}}$):

$$\mathbf{F_{HANDreference}} = m_{crate} * (\mathbf{a}_{crate} - \mathbf{g}) - \mathbf{F_{GRFcrate}}$$

where $\mathbf{g}$ is the gravitational vector ($\mathbf{g} = [\,0 \quad 0 \quad -9.81]$). Crate acceleration was calculated by taking the second derivative of the crate CoM position (center of the crate), tracked by the cluster on the crate.

2.3. Hand force estimation

Hand forces were estimated using three different measurement systems (laboratory, intermediate and ambulatory system). The details of three different measurement systems are described in detail later. For all three systems estimated hand forces ($\mathbf{F_{HANDestimated}}$) were calculated based on the measured GRF ($\mathbf{F_{GRFmeasured\_tot}}$) and the estimated GRF based on the full-body segment accelerations ($\mathbf{F_{GRFestimated\_body}}$). For each sample, $\mathbf{F_{GRFestimated\_body}}$ was calculated based on the mass (m_i) and acceleration of the center of mass ($\mathbf{a}_i$) of each body segment i:

$$\mathbf{F_{GRFestimated\_body}} = \sum_{i=1}^{q} (m_i * (\mathbf{a}_i - \mathbf{g}))$$

were q is the total number of body segments. Subsequently, $\mathbf{F_{HANDestimated}}$ was calculated by subtracting $\mathbf{F_{GRFestimated\_body}}$ (not including the forces due to crate motion and weight) from $\mathbf{F_{GRFmeasured\_tot}}$ (including the external forces of the hands exerted to the crate):

$$\mathbf{F_{HANDestimated}} = \mathbf{F_{GRFmeasured\_tot}} - \mathbf{F_{GRFestimated\_body}}$$

The body was segmented in 16 segments according to Zatsiorsky (Zatsiorsky et al., 1990): pelvis, abdomen, thorax, head, and left and right: thighs, shanks, feet, upper arms, forearms and hands. Individual segment masses were calculated based on segment length and circumference using regression equations reported in the literature (de Leva, 1996; Zatsiorsky, 2002). Subsequently, the estimated segment masses were scaled such that the combined weight of all segments equaled the weight of the subject measured by the FPs.

2.3.1. Laboratory system (OMC + FP)

For the FP and OMC systems the global coordinate system was defined as follows (Fig. 3): anterior-posterior axis pointing forward, the vertical axis pointing upwards and the mediolateral axis pointing sideward. $\mathbf{F_{GRFmeasured\_tot}}$ was calculated by summing the GRFs of the five FPs.

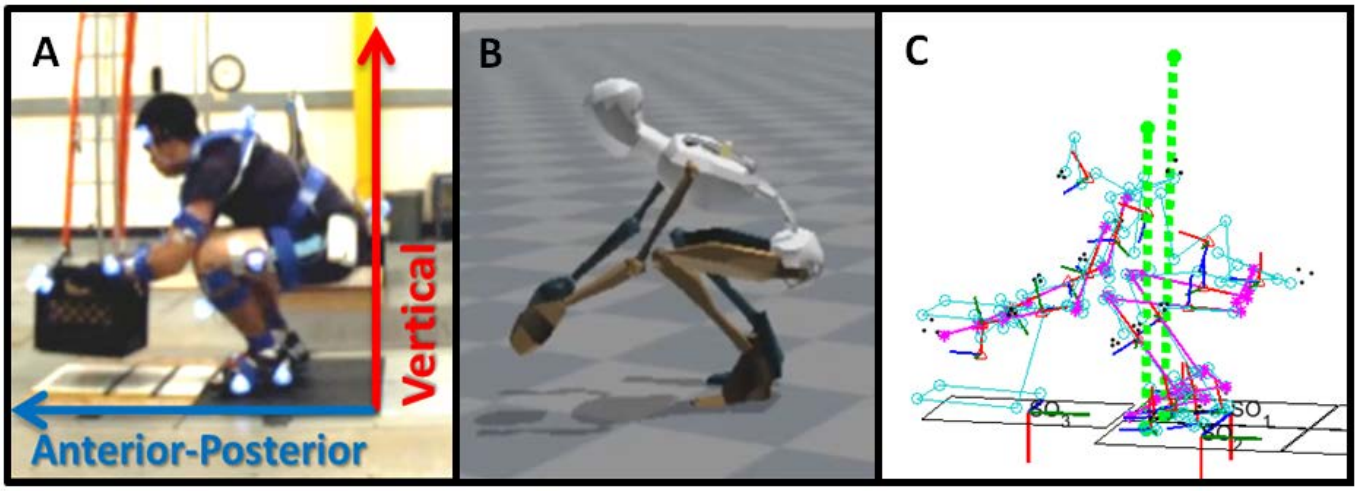

Fig. 3. *(A) Photo of a fully equipped subject lifting the crate. The direction of the anterior–posterior (aligned with the force plate) and vertical axes of the global reference frame are indicated by the arrows. (B) Screenshot of the built-in anatomical body-model of the inertial motion capture (IMC) system (MVN Studio3.0, Xsens technologies B.V., Enschede). (C) Matlab visualization of the 3D inverse dynamics model based on the optical motion capture (OMC) and force plate (FP) data.*

Intermediate system (IMC + FP)

For the OMC, all 16 body segments were tracked using marker clusters. Most segments were tracked by a dedicated marker cluster except for the hands and the abdomen segments. The hands were assumed to be rigidly attached to the forearm segments and the abdomen segment was assumed to be attached to the thorax segment. For all segments, anatomical coordinate systems and center of mass (CoM) positions were calculated based on digitized anatomical landmarks as described in detail elsewhere (Faber et al., 2013b; Faber et al., 2011; Kingma et al., 1996). Segment accelerations ($\mathbf{a}_i$) were obtained by calculating the second derivative of the segment CoM positions.

The intermediate system still used the FP to measure GRFs but the OMC was replaced with the IMC system for measurement of full-body kinematics. For anatomical calibration of the built-in IMC MVN body-model (relating the IMUs to the corresponding segment coordinate systems) an upright calibration posture (N-pose) was recorded (Roetenberg et al., 2013). Furthermore, the model was scaled, based on stature and segment lengths and Kinematic Coupling (KiC^{TM}) algorithm was enabled, to reduce magnetic disturbances of the lower-body kinematics.

The forward axis of the MVN global coordinate system is defined by the direction of the local magnetic north. To align the IMC with the laboratory (OMC+FP) global coordinate systems, all IMC data were rotated about the common vertical axis, such that the heading difference between the OMC and IMC pelvis averaged over time was zero.

To estimate full-body segment CoM positions ($\mathbf{r_{CoM}}$), bony landmark and joint position estimates (including the L5/S1 joint) provided by the built-in MVN body-model were used as input to our 3D model that we also used for the OMC system (same 16 body segments).

MVN provides, based on the IMU inertial recordings, for each segment the angular velocity ($\boldsymbol{\omega}$), angular acceleration ($\boldsymbol{\alpha}$) and the linear acceleration of the origin ($\mathbf{a_{origin}}$) of the segment (usually the proximal joint ($\mathbf{r_{origin}}$) in the earthbound coordinate system. To calculate the segment CoM accelerations ($\mathbf{a_{CoM}}$) the following equation was used for each segment:

$$\mathbf{a_{CoM}} = \mathbf{a_{origin}} + \boldsymbol{\alpha} \times \left(\mathbf{r_{CoM}} - \mathbf{r_{origin}}\right) + \boldsymbol{\omega} \times \left(\boldsymbol{\omega} \times \left(\mathbf{r_{CoM}} - \mathbf{r_{origin}}\right)\right)$$

2.3.2. Ambulatory System (IMC + FS)

The ambulatory system used GRFs measured by the FSs instead of the FPs. In order to rotate the local forces measured by each sensor underneath the FSs to the global OMC coordinate system, forces were first rotated based on the tilt angles measured by the attached IMUs. Subsequently, the forces were rotated about the vertical, using the heading of the corresponding foot as measured by the IMC system (of which the data were already aligned with the OMC data). Finally, $\mathbf{F}_{\mathbf{GRFmeasured\_tot}}$ was obtained by summing the GRFs measured by the four FS sensors in the global coordinate system.

2.4. Data reduction & Statistics

For all 3D HF component time series (vertical, anterior-posterior, mediolateral), the root-mean-squared differences (RMSDs) were determined between the reference HFs and the HFs estimated by the 3 measurement systems (laboratory, intermediate and ambulatory systems). Effects of *Gender* (male, female), *Movement Phase* (lifting, walking, carrying) and *HF Estimation System* (laboratory, intermediate, ambulatory) on HF RMSDs were tested using a three-way mixed analysis of variance (ANOVA). In case of significant main effects of factors with more than 2 levels (*Movement Phase* & *HF Estimation System*), post-hoc paired test were performed. Because also significant *Movement Phase* x *HF Estimation System* interactions were found, *HF Estimation System* effects were tested per *Movement Phase.*

3. Results

3.1. Typical example

Figure 4 shows a typical example (1 subject) of the GRFs and HFs for each of the three *HF Estimation Systems*. The GRFs measured under the feet (FP or FS) includes the forces caused by the crate, while the GRFs estimated based on the motion capture data (OMC or IMC) only includes the body segments. Lifting the crate causes these signals to diverge and the difference provides the estimate of the HFs exerted onto the crate.

3.2. Main effects

Table 1 shows the ANOVA outcomes (p-values). HF errors were significantly affected by *Gender* in the anterior-posterior and mediolateral directions, with slightly smaller HF estimation errors in women. The effects of *Movement Phase* were more substantial and similar for all HF components. Lifting resulted in the lowest RMSDs (7-12N), walking resulted in about 5N higher RMSDs (13-18N), and carrying about 10N higher (18-24N). *HF Estimation Method* had some substantial effects, which varied across the HF components. The smallest HF estimation RMSDs were found for the laboratory system. Replacing the OMC system by the IMC system (intermediate system) resulted in an RMSD increase of about 5N for the anterior-posterior HF component, but no effects were found for the mediolateral and vertical HF components. When the FPs were replaced by the FSs (ambulatory system), RMSDs further increased significantly for all directions, most for the sideways direction (by 6N relative to the intermediate system) and least for the vertical direction (by 2N relative to the intermediate system).

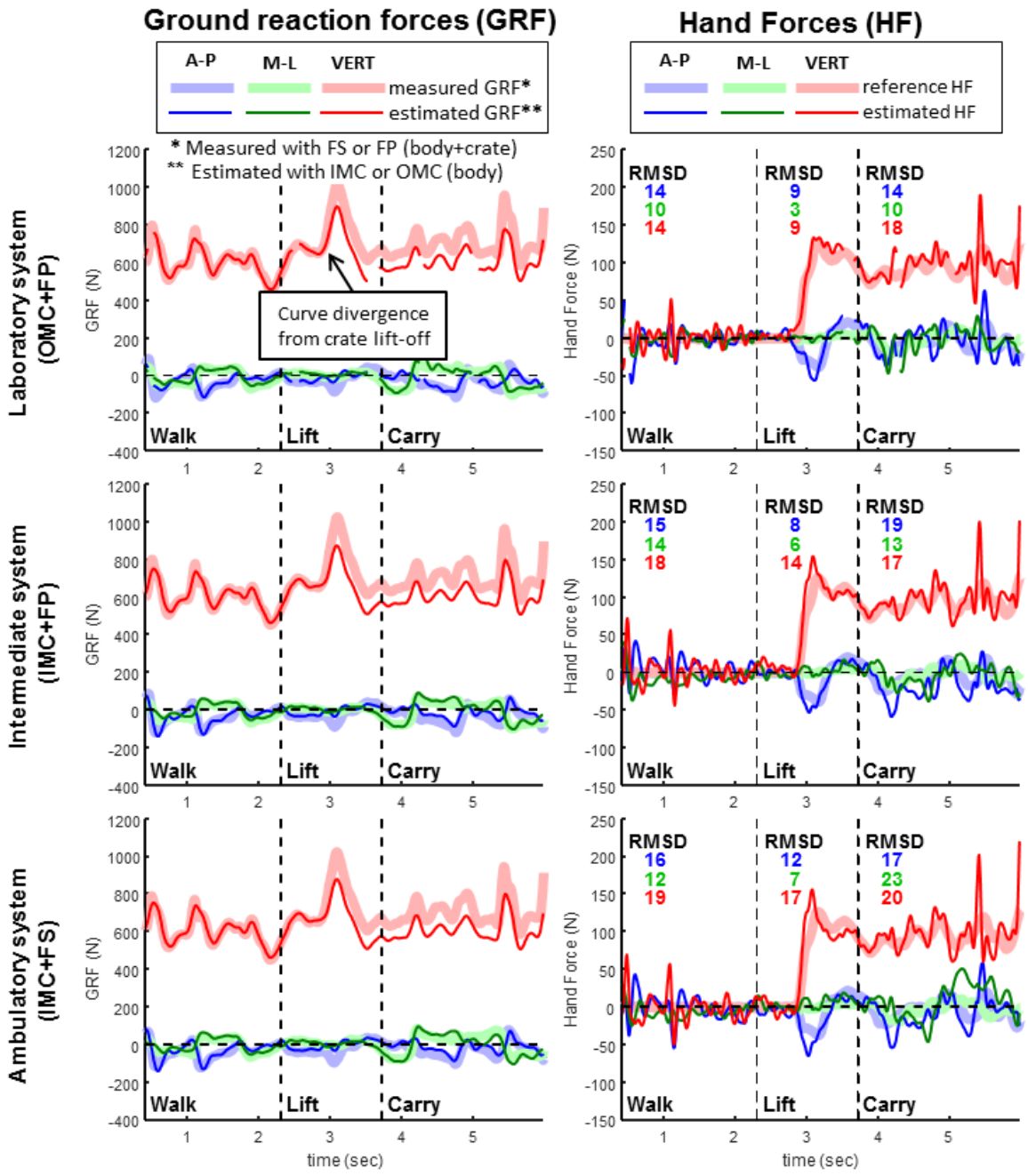

Fig 4. *Typical example (1 subject) of the GRFs and HFs (A-P = anterior-posterior; M-L = mediolateral; VERT=vertical) for each of the three Hand Force Estimation Systems. From the GRFs on the left side it is clear that before crate pick-up (about half way the lifting phase), the measured GRFs (FP or FS) agree well with the GRFs estimated from body segment accelerations (OMC or IMC). From box pick-up the curves start diverging. The difference between measured and estimated GRFS, provides an estimate of the HFs exerted onto the crate, which are shown on the right side together with the reference HFs. The root-mean-square differences (RMSDs) between the estimated and reference HFs are indicated quantifying the effect of Hand Force Estimation System and Movement Phase.*

Table 1. *Results (p-values) of the ANOVA analyses, testing the effects of Hand Force Estimation System (HFES), Movement Phase (MP), Gender (G) and their interactions, on the hand force estimation errors in anterior-posterior (A-P), mediolateral (M-L) and vertical (VERT) directions. Significant effects (p <0.05) are indicated in bold.*

	A-P	M-L	VERT
Hand Force Estimation System (HFES)	**<0.001**	**<0.001**	**0.001**
Movement Phase (MP)	**<0.001**	**<0.001**	**<0.001**
Gender (G)	**0.001**	**0.007**	0.837
HFES x MP	0.722	**0.000**	**0.034**
HFES x G	0.288	0.148	0.797
MP x G	0.797	0.197	0.383
HFES x PM x G	0.354	0.267	0.141

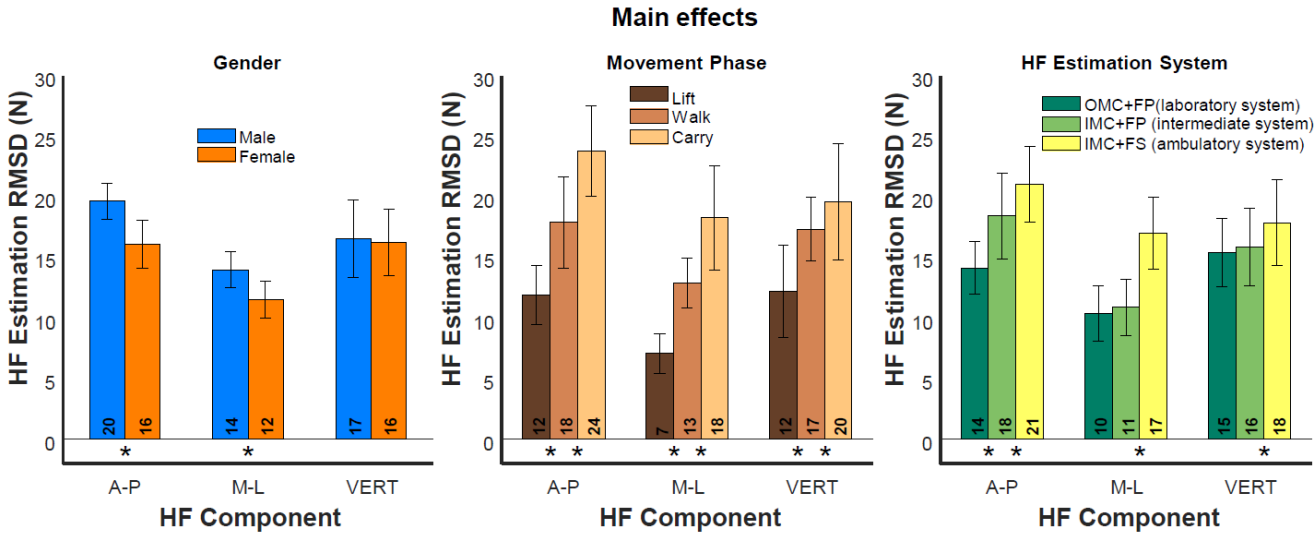

Fig. 5. *Bar plots visualizing the main effects of Gender, Movement Phase, and Hand Force (HF) Estimation System on the HF estimation errors (root-mean-square differences, RMSDs). A-P = anterior-posterior, M-L = mediolateral and VERT = vertical. * indicates a significant difference between adjacent bars. The error bars indicate the standard deviation.*

3.3. Interaction effects

Significant interaction effects of *HF Estimation System x Movement Phase* were found for mediolateral and vertical HFs. Therefore, the effects of *HF Estimation System* were further analyzed per *Movement Phase* (Figure 6). This showed that the effects were qualitatively similar between lifting, walking and carrying.

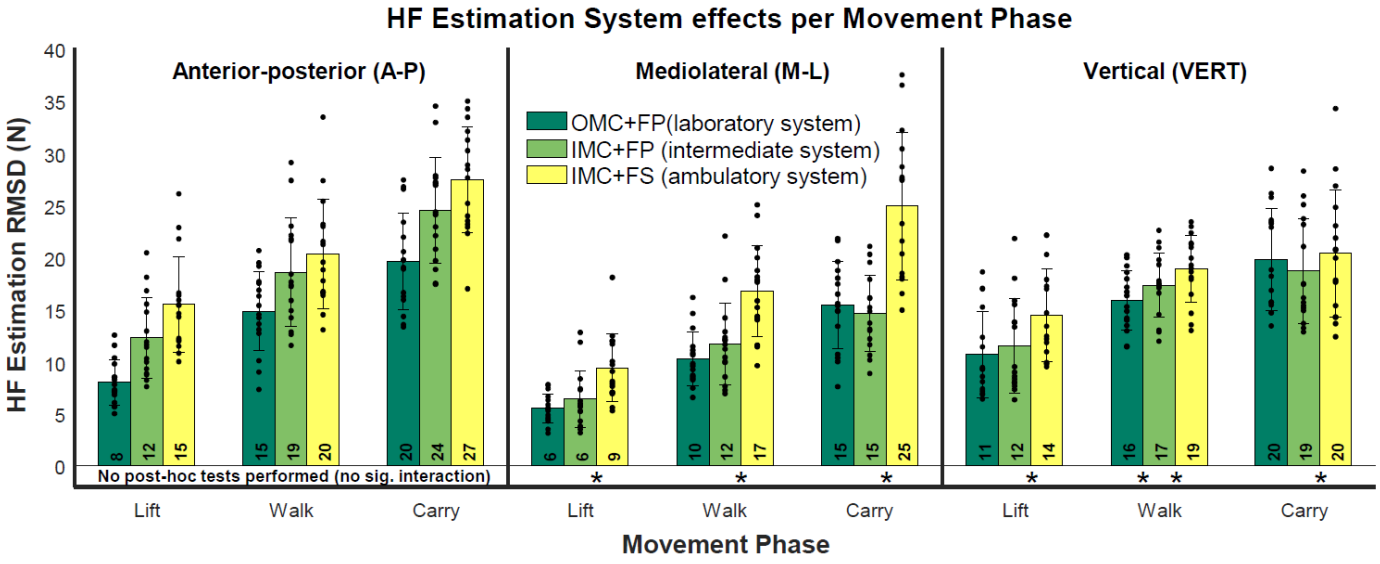

Fig. 6. *Bar plots visualizing the effects of Hand Force (HF) Estimation System on the HF estimation errors (root-mean-square differences, RMSDs) per Movement Phase. * indicates a significant difference between adjacent bars. The error bars indicate the standard deviation. The black dots are the individual RMSD values for all 16 subjects.*

3.4. RMSD error ranges

Averaged over subjects, HF RMSDs across all HF components and movement phases, RMSD error ranges were 6-20N, 6-24N and 10-27N for the laboratory (OMC+FP), intermediate (IMC+FP), and ambulatory (IMC+FSs) systems, respectively. Per movement phase, HF RMSD ranges were 8-11N, 6-12N and 10-15N during lifting, 10-16N, 11-19N and 17-20N during walking, and 15-20N, 15-24N and 20-27N during carrying.

4. Discussion

The aim of the present study was to evaluate 3D hand force (HF) assessment accuracy using an ambulatory measurement system consisting of wearable instrumented force shoes (FSs) measuring ground reaction forces (GRFs), and a full-body inertial motion capture (IMC) suit measuring segment accelerations. The present study showed that HF estimation with the ambulatory measurement system (IMC+FSs) resulted in estimation errors of 10-27N RMSD. Furthermore, lower errors were found during lifting (10-15N RMSD) than during walking (17-20N RMSD) and carrying (20-27N RMSD). This is probably because the feet are stationary during lifting. During walking and carrying, impacts at heel strike might result in incorrect segment acceleration measurement because of relative movement of IMU sensors, due to skin motion artefacts and non-rigidity of the body segments. (Forner-Cordero et al., 2008; Leardini et al., 2005). No major effects of gender were found.

Whether or not the HF errors mentioned above are acceptable, depends on the application of the ambulatory measurement system. As an example, we consider estimating the peak lumbar moments during lifting, using a top-down inverse dynamics model with the HFs as input. Assuming a moment arm of the HFs of about 0.5m (Faber et al., 2007; Kingma et al., 2006), HF errors found for lifting (10-15N RMSD) would result in low back moment errors of 5-7.5Nm. Such errors seem acceptable, since they are small compared to the lumbar peak moments that are typically found during manual lifting, reaching up to 200-300Nm (Faber et al., 2009a). In a study based on the dataset of the current article, the use of the estimated hand forces on spinal loading is further explored (Koopman et al., submitted).

4.1. Sources of error

One potential source of error in HF estimation is related to the measurement equipment. We compared a fully ambulatory system (IMC+FSs) to state-of-the-art laboratory equipment. On average, the laboratory equipment resulted in 30% lower HF estimation errors. To disentangle the errors due to using FSs instead of FPs and using IMC instead of OMC, we also used the intermediate system (IMC+FP). This showed that of the 30% error difference, about 20% was caused by using the FSs

295 instead of the FPs and about 10% was due to using IMC instead of OMC, leaving most of the error
296 (70%) unaccounted for.

297 It is important to realize that the HF errors will not only vary with the type of measurement system
298 used, but also with specific instrumentation within each type. For instance, errors in the laboratory
299 system were 3-4 N smaller than in a previous study, which used another type of FP and another version
300 of the Optotrac system (Faber et al., 2015).

301 Besides measurement errors of the equipment used, another potential error source is that segment
302 CoM accelerations are not captured perfectly by motion sensors (IMUs and marker clusters), due to
303 skin motion artefacts and due to the fact that human body segments are not rigid. Also, mass
304 distribution and center of mass location in participants may differ from the anthropometric model
305 used to estimate these parameters, which may affect errors as well. Unfortunately, it is not possible to
306 find out how the remaining 70% of error is distributed over such error sources.

307

308 *4.2. Limitations*

309 Several limitations need to be considered. First, mostly young healthy subjects participated and motion
310 sensors were placed directly on the skin. HF errors might increase when there is more motion of IMU's
311 relative to the bone, such as in obese subjects or when IMUs are worn on top of clothes, as estimates
312 of segment CoM accelerations will be less accurate.

313 Second, because the ambulatory system relies on IMU orientations, which use the earth magnetic field
314 to determine their orientation about the global vertical (heading), the HF accuracy in the horizontal
315 plane, anterior-posterior and mediolateral HF (not the vertical HF), may be affected by magnetic
316 disturbances due to nearby metal objects or electromagnetic fields. In the present study, we
317 attempted to minimize these effects to determine system performance in an optimal situation. To
318 accomplish this, subjects started each measurement on a wooden platform. However, during the lifts
319 subjects moved through a magnetically disturbed volume with the FPs, but since these distortions
320 were temporary, the Xsens IMU fusion Kalman filters and KiC algorithm could compensate for these
321 disturbances. It is unclear how our ambulatory system will perform in an environment with more

continuous magnetic distortions. However, recent studies found that the Xsens system shows good resilience against more continuous magnetic disturbances (Kim and Nussbaum, 2013; Robert-Lachaine et al., 2017) and therefore, the effects of magnetic disturbances on HF estimation are probably minimal.

Third, we only focused on lifting/carrying a 10kg crate from ground level. This initial crate location was chosen because it results in high segment accelerations. Lifting from less extreme locations will probably lead to smaller segment accelerations and therefore smaller HF errors. However, the system performance still needs to be tested in other manual material handling tasks such as pushing and pulling.

Fourth, our reference hand forces were not measured directly but calculated based on crate kinematics and GRF data from a FP that the crate was lifted from. However, the accuracy of this method was probably sufficient since the HF errors of the laboratory system (OMC+FP) were comparable or even a bit lower than the HF errors found for the laboratory system in a previous study where HFs were directly measured with an instrumented crate (Faber et al., 2013a).

Fifth, we made use of a specific build-in body-model provide by the Xsens MVN software, which compensates for the magnetic disturbances by the build-in Kalman and KiC algorithms and the body-model. Results may not generalize to other IMC systems.

Finally, the current method assumes that all the external forces are exerted by the hands (HF) and the feet (GRF), as was the case during the experiment. In practice, subjects might also exert forces onto the environment with other body parts, for example when leaning against a railing while lifting. In these cases, our HF estimation method will calculate the sum of the hand and waist forces, but cannot distinguish between these forces.

4.3. Conclusion

In conclusion, the current study showed that estimating hand forces using an ambulatory measurement system, consisting of a full body inertial motion capture and instrumented force shoes, resulted in hand force estimation errors from 10-27N. This error is regarded acceptable for the assessment of spinal loading during manual lifting. Future studies should investigate the system performance using a wider variety of tasks.

Conflict of interest statement

The authors state that there is no conflict of interest to report.

Acknowledgment

The authors thank Mr. Jacob Banks and Mr. Niall O'Brien at Liberty Mutual Research Institute for Safety for assistance during data collection. This work was supported by the European Union's Horizon 2020 through the SPEXOR project, contract no. 687662 and partly by the Liberty Mutual - Harvard T.H. Chan School of Public Health postdoctoral program.

References

- Coenen, P., Kingma, I., Boot, C.R., Faber, G.S., Xu, X., Bongers, P.M., van Dieen, J.H., 2011. Estimation of low back moments from video analysis: A validation study. Journal of Biomechanics 44, 2369-2375.
- Coenen, P., Kingma, I., Boot, C.R.L., Twisk, J.W.R., Bongers, P.M., van Dieen, J.H., 2013. Cumulative Low Back Load at Work as a Risk Factor of Low Back Pain: A Prospective Cohort Study. Journal of Occupational Rehabilitation 23, 11-18.
- de Leva, P., 1996. Adjustments to Zatsiorsky-Seluyanov's segment inertia parameters. Journal of Biomechanics 29, 1223-1230.
- Dennis, G.J., Barrett, R.S., 2002. Spinal loads during individual and team lifting. Ergonomics 45, 671-681.
- Faber, G.S., Kingma, I., van Dieen, J.H., 2007. The effects of ergonomic interventions on low back moments are attenuated by changes in lifting behaviour. Ergonomics 50, 1377-1391.
- Faber, G.S., Kingma, I., Kuijer, P.P., van der Molen, H.F., Hoozemans, M.J., Frings-Dresen, M.H., van Dieen, J.H., 2009a. Working height, block mass and one- vs. two-handed block handling: the contribution to low back and shoulder loading during masonry work. Ergonomics 52, 1104-1118.
- Faber, G.S., Kingma, I., Martin Schepers, H., Veltink, P.H., van Dieen, J.H., 2009b. Determination of joint moments with instrumented force shoes in a variety of tasks. Journal of Biomechanics 43, 2848-2854.
- Faber, G.S., Kingma, I., van Dieen, J.H., 2011. Effect of initial horizontal object position on peak L5/S1 moments in manual lifting is dependent on task type and familiarity with alternative lifting strategies. Ergonomics 54, 72-81.
- Faber, G.S., Chang, C.C., Kingma, I., Schepers, H.M., Herber, S., Veltink, P.H., Dennerlein, J.T., 2012. A force plate based method for the calibration of force/torque sensors. Journal of Biomechanics 45, 1332-1338.
- Faber, G.S., Chang, C.C., Kingma, I., Dennerlein, J.T., 2013a. Estimating dynamic external hand forces during manual materials handling based on ground reaction forces and body segment accelerations. Journal of Biomechanics 46, 2736-2740.
- Faber, G.S., Chang, C.C., Kingma, I., Dennerlein, J.T., 2013b. Lifting style and participant's sex do not affect optimal inertial sensor location for ambulatory assessment of trunk inclination. Journal of Biomechanics 46, 1027-1030.
- Faber, G.S., Chang, C.C., Kingma, I., Dennerlein, J.T., van Dieen, J.H., 2015. Estimating 3D L5/S1 moments and ground reaction forces during trunk bending using a full-body ambulatory inertial motion capture system. Journal of Biomechanics.
- Forner-Cordero, A., Mateu-Arce, M., Forner-Cordero, I., Alcantara, E., Moreno, J.C., Pons, J.L., 2008. Study of the motion artefacts of skin-mounted inertial sensors under different attachment conditions. Physiol Meas 29, N21-N31.
- Kim, S., Nussbaum, M.A., 2013. Performance evaluation of a wearable inertial motion capture system for capturing physical exposures during manual material handling tasks. Ergonomics 56, 314-326.
- Kingma, I., de Looze, M.P., Toussaint, H.M., Klijnsma, H.G., Bruijnen, T.B.M., 1996. Validation of a full body 3-D dynamic linked segment model. Human Movement Science 15, 833-860.

- Kingma, I., Faber, G.S., Bakker, A.J.M., van Dieën, J.H., 2006. Can low back loading during lifting be reduced by placing one leg beside the object to be lifted? Physical Therapy 86, 1091-1105.
- Koopman, A.S., Kingma, I., Faber, G.S., Bornmann, J., Dieën, J.H.v., submitted. Estimating 3D L5S1 moments using a simplified ambulatory measurement system. Journal of Biomechanics (this special issue).
- Leardini, A., Chiari, L., Della Croce, U., Cappozzo, A., 2005. Human movement analysis using stereophotogrammetry - Part 3. Soft tissue artifact assessment and compensation. Gait & Posture 21, 212-225.
- Liedtke, C., Fokkenrood, S.A.W., Menger, J.T., van der Kooij, H., Veltink, P.H., 2007. Evaluation of instrumented shoes for ambulatory assessment of ground reaction forces. Gait & Posture 26, 39-47.
- Marras, W.S., Lavender, S.A., Ferguson, S.A., Splittstoesser, R.E., Yang, G., Schabo, P., 2010. Instrumentation for measuring dynamic spinal load moment exposures in the workplace. Journal of Electromyography and Kinesiology 20, 1-9.
- Plamondon, A., Gagnon, M., Desjardins, P., 1996. Validation of two 3-D segment models to calculate the net reaction forces and moments at the L(5)/S-1 joint in lifting. Clinical Biomechanics 11, 101-110.
- Plamondon, A., Lariviere, C., Denis, D., Mecheri, H., Nastasia, I., Grp, I.M.R., 2017. Difference between male and female workers lifting the same relative load when palletizing boxes. Applied Ergonomics 60, 93-102.
- Robert-Lachaine, X., Mecheri, H., Larue, C., Plamondon, A., 2017. Effect of local magnetic field disturbances on inertial measurement units accuracy. Applied Ergonomics 63, 123-132.
- Roetenberg, D., Luinge, H.J., Slycke, P., 2013. Xsens MVN: Full 6DOF Human Motion Tracking Using Miniature Inertial Sensors. Xsens Technologies B.V, 1-5.
- Schepers, H.M., Koopman, H.F.J.M., Veltink, P.H., 2007. Ambulatory assessment of ankle and foot dynamics. IEEE Transactions on Biomedical Engineering 54, 895-902.
- Veltink, P.H., Liedtke, C., Droog, E., van der Kooij, H., 2005. Ambulatory measurement of ground reaction forces. IEEE Transactions on Neural Systems and Rehabilitation Engineering 13, 423-427.
- Zatsiorsky, V.M., Seluyanov, V.N., Chugunova, L.G., 1990. Methods of determining mass-inertial characteristics of human body segments, in: Chemyi G. G. and Regirer, S.A. (Ed.), In Contemporary Problems of Biomechanics. CRC Press, Massachusetts, pp. 272-291.
- Zatsiorsky, V.M., 2002. Kinetics of human motion. Human Kinetics, Champaign, IL, pp. 605-611.